The dissociative recombination of OH^+

Steven L. Guberman
Institute for Scientific Research, 33 Bedford Street, Lexington, Massachusetts 02173

(Received 15 August 1994; accepted 17 October 1994)

Theoretical quantum chemical calculations of the cross sections and rates for the dissociative recombination of the $v=0$ level of the ground state of OH^+ show that recombination occurs primarily along the $2\,^2\Pi$ diabatic route. The products are $O(^1D)$ and a hot H atom with 6.1 eV kinetic energy. The coupling to the resonances is very small and the indirect recombination mechanism plays only a minor role. The recommended value for the rate coefficient is $(6.3\pm0.7)\times10^{-9}\times(T_e/300)^{-0.48}$ cm^3/s for $10<T_e<1000$ K. © *1995 American Institute of Physics.*

I. INTRODUCTION

The dissociative recombination (DR) of OH^+,

$$OH^+ + e^- \rightarrow O + H, \tag{1}$$

is an important reaction in a number of settings. OH^+ has been detected in comets[1] at concentrations comparable to H_2O^+ and H_3O^+.[2] The Pioneer 11 and Voyager 1 and 2 spacecraft have detected OH^+ in the plasma torus of Saturn. A model[3] has shown that DR of OH^+ can limit the ion densities near several Saturnian moons and lead to a large outflow of neutrals which can escape from the magnetosphere. DR of OH^+ has been included in a model of the magnetosphere of Uranus.[4] These environments are difficult to model because the DR rate constant for OH^+ has never been measured directly or calculated. The only prior work was a merged beam measurement[5] of the cross section starting at about 0.003 eV electron energy. The reported cross sections were smaller than those found for other diatomics and it was remarked that the low cross section could be due to an unfavorable crossing of ion and dissociative curves.

The *ab initio* calculation of the DR cross sections and rates for (1) involves three distinct steps. First, accurate potential curves are required for the description of the nuclear motion in the exit channel of reaction (1) and within the bound ion in the entrance channel. The nuclear motion in the exit channel occurs on a diabatic state. The calculation of diabatic states differs slightly from the approach used for fully optimized states and this is discussed further below. In the second step, we calculate the coupling between the electron–ion continuum in the entrance channel and the nuclear motion continuum in the exit channel. In direct DR,[6] we confine our attention solely to the interaction of the two continua in reaction (1). The direct DR cross section can be calculated from a simple expression[7] if there is only a single important dissociative channel for each molecular state symmetry. There are, however, neutral vibrationally excited Rydberg states that interact with both continua and act as intermediate states in recombination. Once excited, they can autoionize back to the ion plus a free electron or predissociate along the exit channel. The Rydberg levels drive indirect DR.[8] In many molecules, these intermediate states can greatly affect the magnitude of the cross section. In the third step, the Rydberg levels and the two continua are included simultaneously in a multichannel quantum defect theory (MQDT) calculation of the cross sections and rates.[7,9]

In the next section, we discuss the repulsive states that describe the nuclear motion on the right side of reaction (1). Section III describes the construction of the diabatic wave functions. The direct DR cross section and the calculation of the electron capture widths is contained in Sec. IV. The calculation of the quantum defects is described in Sec. V. The full MQDT calculations for the cross sections and rates are discussed in Sec. VI.

II. DR MECHANISM FOR OH^+

In order for the rate of reaction (1) to be high in a diabatic description, it is necessary to have a potential curve describing the motion in the exit channel [the right side of reaction (1)] cross the ion potential curve within the classical turning points of the vibrational level of interest (for DR involving adiabatic potential curves see Ref. 10).[11] If there is also a favorable electronic capture width, a favorable diabatic crossing situation assures a high Franck–Condon factor between the two channels and a high direct recombination cross section.[6] This is discussed further in Sec. IV. Three asymptotes of the valence separated atoms, $O(^3P)+H(^2S)$, $O(^1D)+H(^2S)$,$O(^1S)+H(^2S)$ are at 8.5, 6.5, and 4.7 eV,[12,13] respectively, below the $v=0$ level of the $^3\Sigma^-$ ion ground state. The lowest asymptote, $O(^3P)+H(^2S)$, gives molecular states of $^{4,2}\Pi$, and $^{4,2}\Sigma^-$ symmetry. The $^2\Pi$ state is the ground state of OH and it does not cross the ion. The $O(^1D)+H(^2S)$ asymptote gives $^2\Delta$, $^2\Pi$, and $A\,^2\Sigma^+$ states. The A state is well known and does not cross the ion. Furthermore, because of the + symmetry, it can only have a negligible electron capture width. The highest asymptote, $O(^1S)+H(^2S)$ at 4.7 eV, leads to a $^2\Sigma^+$ state which can also be neglected. The lowest Rydberg asymptote, $O(^5S)+H(^2S)$, lies 0.7 eV above the $v=0$ level of the ion. Therefore, only five states are possible routes for DR from the low vibrational levels of OH^+ at low electron energies.

III. WAVE FUNCTIONS

The potential curves for the ion and neutral states were determined from large scale wave functions expanded in Gaussian basis functions. The basis set on the O was constructed from the $13s$, $8p$ primitive set of van Duijneveldt[14] with exponents rounded to no more than seven significant

figures. The oxygen exponents[15] for the even tempered $(6d, 4f, 2g)$ polarization set, α_k^i, are generated from $\alpha_k^i=\beta_i/(2.5)^k$ where $i=d,f,g$, $\beta_d=12.65$, $\beta_f=6.07$, $\beta_g=3.11$ with k running from 0 to n_i-1 where n_i is the number of basis functions of each type. These exponents were rounded to two decimal places. The contraction coefficients for the $[5s,4p,3d,2f,1g]$ set were obtained from the natural orbitals derived from an oxygen atom singles and doubles CI calculation as described by Almlöf and Taylor.[16] On the H, an 8 s set of van Duijneveldt[14] was supplemented by $6p$ and $4d$ polarization functions with $\beta_p=9.88$ and $\beta_d=4.0$. The polarization exponents were rounded to two decimal places. The primitive set on the H was contracted to a $[4s,3p,2d]$ set with coefficients obtained from the natural orbitals for H_2.[16] Diffuse basis functions on the O for the description of negative ion or Rydberg character were intentionally omitted since the dissociative states determined here must be diabatic valence states (see below).

For the $^3\Sigma^-$ ground state of the ion, the orbitals were determined in complete active space self-consistent field[17] (CASSCF) calculations. The primary configuration of the ion ground state is $1\sigma^2 2\sigma^2 3\sigma^2 1\pi_x 1\pi_y$. The configurations for the CASSCF were determined by taking all excitations within the space of the 3σ, 4σ, 5σ, and the 1π, and 2π orbitals. The 1σ and 2σ orbitals were constrained to be doubly occupied. This generated a 56 term wavefunction. The calculations were done in C_{2v} symmetry but $C_{\infty v}$ symmetry was imposed upon the orbitals. A configuration interaction[18] (CI) wave function was generated by taking all single and double excitation to the virtual orbitals from each of the 56 terms of the CASSCF wave function with the restriction that the 1σ orbital remain doubly occupied. This procedure generated a 378 706 term wave function. All energies reported here include the multireference analog of the Davidson correction for missing quadrupole excitations.[19] The calculated energies are listed in Table I and the spectroscopic constants are given in Table II where they are compared with prior calculations. The calculated equilibrium internuclear separation differs from experiment by only 0.0015 a_0 and ω_e differs by only 6 cm^{-1}. The calculated electronic dissociative energy is 0.14 eV smaller than experiment because the CI description of O in the $O+H^+$ limit is better than the description near R_e.

For the neutral $^{4,2}\Pi$, $^{4,2}\Sigma^-$, and $^2\Delta$ states, wave functions were constructed using the same procedure as for the ion. Optimum orbitals were determined for each symmetry. For the $^2\Pi$ states, the orbitals were an average of those for the lowest two $^2\Pi$ states. Also, in the calculations on $^2\Sigma^-$ and $^2\Delta$ states the orbitals used were averaged for these two states. Exploratory calculations were done on each of these states to see if any diabatic state crossed within the turning points of the $v=0$ ion level. The calculations in $^2\Pi$ symmetry give the neutral ground state as the first root. The calculated ionization potential of the $v=0$ level of the $^2\Pi$ ground state is 12.9427 eV and compares quite well to the experimental value of 12.90 eV.[12] The other spectroscopic constants are reported in Table II. The calculated R_e differs from experiment by only 0.0036 a_0 and ω_e differs by only 19 cm^{-1}. The electronic dissociation energy is only 0.02 eV smaller than experiment. The calculated spectroscopic constants for $X\ ^2\Pi$ are quite similar to those given by prior[20] high quality calculations which explored several one particle and n-particle approaches. The earlier calculations used a nearly identical basis set to that used here supplemented with additional dif-

TABLE I. Calculated CI energies for the ground states of OH^+, OH, and the $2\ ^2\Pi$ state of OH. Add -75.0 to the listed energies to get the total energy.

$R(a_0)$	$X\ ^3\Sigma^-$	$X\ ^2\Pi$	$2\ ^2\Pi$
1.3	−0.009 189	−0.515 534	0.049 761
1.4	−0.079 973	−0.581 020	−0.024 915
1.5	−0.126 994	−0.622 871	−0.078 366
1.6	−0.157 245	−0.648 084	−0.118 140
1.7	−0.175 632	−0.661 569	−0.149 937
1.8	−0.185 622	−0.666 783	−0.177 950
1.9	−0.189 686	−0.666 171	−0.204 825
2.0	−0.189 593	−0.661 595	−0.230 339
2.1	−0.186 615	−0.654 335	−0.254 670
2.2	−0.181 670	−0.645 327	−0.277 409
2.3	−0.175 421	−0.635 258	−0.298 188
2.4	−0.168 347	−0.624 633	−0.316 859
2.5	−0.160 812	−0.613 824	−0.333 429
2.6	−0.153 081		
2.7	−0.145 332	−0.592 668	−0.360 689
2.8	−0.137 684	−0.582 668	−0.371 680
2.9	−0.130 221	−0.573 208	−0.381 131
3.0	−0.122 997	−0.564 361	−0.389 203
3.2	−0.109 388	−0.548 679	−0.401 806
3.4	−0.096 976	−0.535 780	−0.410 576
3.6	−0.085 758	−0.525 578	−0.416 437
3.8	−0.075 672	−0.517 799	−0.420 171
4.0	−0.066 635	−0.512 055	−0.422 431
4.2	−0.058 558		
4.4	−0.051 352	−0.504 978	−0.424 441
4.6	−0.044 935	−0.502 912	−0.424 813
4.8	−0.039 233		
5.0	−0.034 178	−0.500 443	−0.425 087
5.5	−0.023 962	−0.499 018	−0.425 130
6.0	−0.016 503	−0.498 405	−0.425 102
6.5	−0.011 114	−0.498 131	−0.425 065
7.0	−0.007 304	−0.498 003	−0.425 033
7.4		−0.497 949	−0.425 013
7.6	−0.004 285	−0.497 932	−0.425 005
7.8	−0.003 584	−0.497 919	−0.424 998
8.0	−0.003 015	−0.497 908	−0.424 992

TABLE II. OH spectroscopic constants.

$OH^+\ X\ ^3\Sigma^-$	a	b	This work	Experimental[c]
$R_e(a_0)$	1.948	1.9517	1.9458	1.9443
D_e (eV)	5.358	5.31	5.14	5.28
ω_e (cm^{-1})	3088.1	3104	3119	3113
$\omega_e x_e$ (cm^{-1})	72.8	77.8	83.67	78.52
OH $X\ ^2\Pi$	MRCI[d]	ACPF[d]	This work	Experimental[c]
R_e (a_0)	1.838	1.836	1.8360	1.8324
D_e (eV)	4.589	4.593	4.605	4.62
ω_e (cm^{-1})			3756	3737
$\omega_e x_e$ (cm^{-1})			111.23	84.88

[a]R. P. Saxon and B. Liu, J. Chem. Phys. **85**, 2099 (1986).
[b]D. M. Hirst and M. F. Guest, Mol. Phys. **49**, 1461 (1983).
[c]Reference 12.
[d]Reference 20.

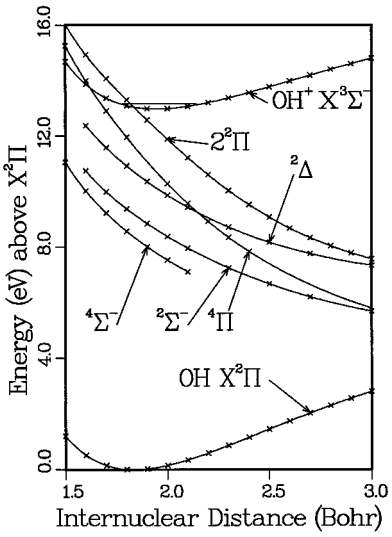

FIG. 1. The calculated potential curves for the ground state of OH^+ and the neutral diabatic states of OH. The calculated points are shown by an x. The $v=0$ vibrational level is included in the ion potential well.

fuse functions needed for an accurate description of the dipole moment function. A smaller reference space was used for generating the multireference CI (MRCI) wave function than that used here. Results were also reported using the averaged coupled-pair functional method (ACPF). The prior results for R_e and D_e are compared with the results reported here in Table II.

From Fig. 1, the only state identified as a likely route for DR is the $2\,^2\Pi$ state which crosses the ion near the inner turning point of the $v=0$ level. The calculated electronic excitation energy of the diabatic $2\,^2\Pi$ state at 1.8 a_0 is 13.30 eV compared to 13.09 eV for the ion. For the $^2\Sigma^-$, $^2\Delta$, $^4\Sigma^-$, and $^4\Pi$ diabatic states, the excitation energies at 1.8 a_0 are 9.37, 10.91, 8.56, and 11.94 eV. All of these repulsive states fall under the ion at internuclear distances that are between the turning points of the $v=0$ level. The calculated energies for the $^2\Pi$ states are given in Table I.

The excited neutral states have been the subject of several prior calculations.[21] However, the prior calculations are adiabatic calculations in which the states are allowed to mix in Rydberg character. If a good description of Rydberg character is provided, none of these optimized adiabatic states can cross the ion because of the noncrossing rule. Here, we are interested in diabatic states which cross the ion and can provide routes for DR. These states can be formulated by projecting out the ground state of the ion from the neutral adiabatic states. While this can be done exactly for the case of the DR of H_2^+ or other one electron ions,[22] it cannot be done exactly for many electron ions. In the calculations reported here, this projection is approximated by not including Rydberg character in the diabatic wave functions. These diabatic curves with high excitation energies will usually be more repulsive with respect to the ground state than comparable adiabatic states. The only exceptions are cases for which Rydberg character is not energetically important. Our results indicate, as expected, that this is clearly the case for the ground states of the neutral and the ion where the spectroscopic constants are in excellent agreement with experimentally derived results.

All potential curve calculations reported here were done with the MOLECULE-SWEDEN programs.[23]

IV. DIRECT DR CROSS SECTION AND RESONANCE WIDTHS

The cross section for direct DR, i.e., for capture only into the dissociative state without considering the intermediate neutral Rydberg levels, is approximately proportional to an electron capture width. The expression for the direct DR cross section from ion vibrational level v along a single dissociative route is given by[7]

$$\sigma_v=\left(\frac{\pi r}{2k_e^2}\right)\frac{4\xi_v}{(1+\Sigma_{v'}\xi_{v'})^2}, \tag{2}$$

where r is the ratio of the dissociative state statistical weight to that for the ion. The factor of 2 accounts for the electron spin, k_e is the electron wave number, and the summation over v' runs over all $v'\leqslant v$. The ξ_v are given by

$$\xi_v=\left(\frac{\pi}{2}\right)[\langle X_d|\Gamma^{1/2}(R)|X_v\rangle]^2 \tag{3}$$

where X_d and X_v are the continuum and bound vibrational wave functions for the dissociative and electron–ion states, respectively. The internuclear distance (R) dependent electronic width is given by

$$\Gamma(R)=2\pi\rho\langle\{\Phi_{\text{ion}}(x,R)\phi_r(x,R)\}|H|\Phi_d(x,R)\rangle^2, \tag{4}$$

where ρ is a density of states. The brackets on the left side of the matrix element denote the antisymmetrized product of a multielectron wave function for the ion with that for the Rydberg electron, ϕ_r. H denotes the Hamiltonian operator and Φ_d labels the multiconfiguration wave function for the dissociative state. The integration is done over the electronic coordinates, x.

The electronic widths are not only essential to the direct recombination cross section but they also play an important role in connecting the entrance channel in DR to excited Rydberg vibrational levels via a second order electronic coupling.[9] The widths are calculated by using a large diffuse Gaussian basis set to represent high principal quantum number, n, Rydberg orbitals. Because of the tight valence state on the right side of the matrix element in Eq. (4), only the portion of the Rydberg orbital close to the molecule contributes to the integral. Close to the molecule, the high n Rydberg orbital is quite similar to a "free" continuum Coulomb orbital except for the normalization which we take into account with the ρ factor in Eq. (4). It would be prohibitively expensive and impractical to use wave functions of the scale used for the potential curves in the calculation of high Rydberg states. Because of this we use much smaller valence basis sets for the width calculations. A $[3s,2p,1d]$ contracted basis set on the O and a $[2s,1p]$ basis on the H are used for representing the valence orbitals. The basis set on the O was contracted from a $(9s,4p,2d)$ set.[24,25] The s H basis is a contraction of a $(4s)$ set[24] and the p basis function

is a single $2p$ primitive with an exponent of 1.0. Eighteen diffuse $2p_x$ and 18 diffuse $3d_{xz}$ functions were used to represent the high Rydberg orbitals with exponents, $\alpha(n,l)$, taken from Kaufmann *et al.*[26] using the expression $\alpha(n,l)=(1/2n^2)(1/(a_l n+b_l))^2$ where $a_1=0.452\,615$ and $b_1=0.309\,805$ for the $2p_x$ exponents and $a_2=0.382\,362$ and $b_2=0.251\,333$ for the $3d_{xz}$ exponents. n ranged from 1.5 to 10.0 at 0.5 steps in both cases. For this range of n values we are able to obtain good descriptions of Rydberg orbitals up to principal quantum number 10 and the $n=10$ Rydberg orbital was used for the calculation of the widths. The Rydberg orbital was determined in improved virtual orbital (IVO)[27] calculations in $^2\Pi$ symmetry. The calculated width is a capture width for a zero energy electron. Because of the coulomb potential, these widths are expected to vary only slowly with electron energy. The capture widths are expected to be adequate for describing low electron energy DR.

For the multiconfiguration wave functions used in the width calculations, the valence orbitals were optimized in CASSCF calculations on the ground state of the ion having the 2σ, 3σ, 4σ, 1π, and 2π orbitals active. The 1σ orbital was kept doubly occupied. The valence orbitals determined here were used to represent both the ion and $2\,^2\Pi$ state in the width calculations for the $2\,^2\Pi$ state. Using the ion orbitals, a small multiconfiguration wave function for the valence $^2\Pi$ states was constructed by taking all single and double excitations from the most important configurations of the X and valence $2\,^2\Pi$ states: $1\sigma^2 2\sigma^2 3\sigma^2 1\pi^3$ and $1\sigma^2 2\sigma^2 3\sigma 4\sigma 1\pi^3$. The orbital space included those listed in these configurations plus the 2π orbital. Restricting the 1σ orbital to be doubly occupied, this procedure generated 77 spin eigenfunctions. The Rydberg CI wave function reference set has three configurations consisting of the main configuration for the ion wave function, $1\sigma^2 2\sigma^2 3\sigma^2 1\pi^2$, plus a single electron in either the valence virtual 3π or 4π or the Rydberg π orbital determined above. Taking all single and double excitations within the same orbital space used in the valence CI but restricting the group of 3π, 4π, and Rydberg π orbitals to have no more than a single electron generated 75 configurations or 249 spin eigenfunctions. Using a procedure that has been described previously,[28,29] the neutral valence Hamiltonian matrix was transformed to eliminate the two low lying $^2\Pi$ roots. The remaining roots in the $^2\Pi$ space were allowed to mix into the Rydberg space, providing additional correlation. Therefore, the final Rydberg space wave function is $249+77-2=324$ terms in length. The Hamiltonian matrix element with the 77 term valence wave function for $2\,^2\Pi$ yielded the electronic capture width [Eq. (4)]. The calculated widths are quite small and are shown as the solid line in Fig. 2. The calculated value at $R=2.2\ a_0$ is only 0.012 eV for "l"$=1$ and only 0.000 88 eV for the "l"$=2$ Rydberg orbital. The "l"$=2$ Rydberg orbital is nonpenetrating and in the IVO calculations it has a very small quantum defect of only 0.024 compared to that for "l"$=1$ of 0.73. The $3d$ basis functions in the "l"$=1$ Rydberg orbital were found to play only a small role, decreasing the value of the width by only 0.0007 eV. We have therefore neglected the "l"$=2$ contribution and in the calculation of the cross section we only us a single

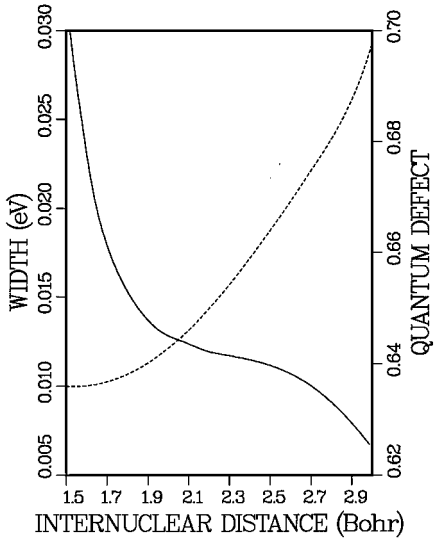

FIG. 2. The calculated electron capture widths (solid line) and the quantum defects (dashed line).

"l"$=1$ partial wave for the free electron. The small widths calculated here indicate that both the direct recombination rate coefficient and the second order electronic coupling[9] to the Rydberg states are small. As a rough indication of the expected accuracy of these small widths, we refer to our calculation of the small width of the $1\,^3\Pi_g$ state of O_2 which differed from an experimentally derived value by only a few percent.[28]

The calculated Rydberg wave function is based on a 25 configuration ion wave function which has an R_e of 1.9604 a_0 or 0.0146 a_0 larger than the R_e calculated for the ion curve in Sec. III. In order to make the widths consistent with the ion curve used in the cross section calculations, the widths have been shifted to smaller R by 0.0146 a_0.

In separate test calculations, we found that the use of $2\,^2\Pi$ optimized CASSCF orbitals instead of ion orbitals, decreased the final calculated width by about 20%. This variation of the width with the nature of the orbitals is taken into account in determining the recommended value for the rate given in Sec. VI.

V. QUANTUM DEFECT

In the full cross section calculation, the variation of the quantum defect with R provides a measure of the coupling between the incoming electron and the nuclear motion. This coupling describes the Born–Oppenheimer breakdown contribution to indirect recombination.[7,30] For the calculation of the quantum defect, all single and double excitations within the 2σ–4σ, 1π, and 2π orbitals were generated from the main ion configuration giving 25 configurations and 47 spin eigenfunctions. The Rydberg wave function was generated by adding to each of these configurations one of the 1π–4π valence orbitals or the Rydberg $n=3$ π orbital. This generated 112 configurations and 332 spin eigenfunctions. The quantum defect was calculated from the energy difference between the ion state and the second root corresponding to

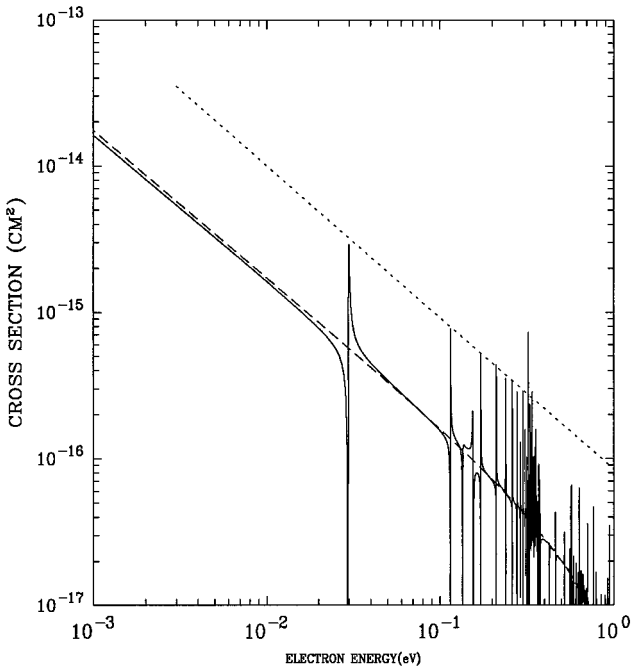

FIG. 3. The direct recombination cross section (dashed line) and the full cross section (solid line) are shown with the line (small dashes) reported as a fit to the points in the merged beam results.

the $n=3$ Rydberg state. The quantum defects are shown as the dashed line in Fig. 2. In addition to the widths, the quantum defects have been shifted to smaller R by 0.0146 a_0. In the region of the ion minimum, $d\mu/dR$ is quite small, 0.016 a_0^{-1}, relative to other molecules studied in this laboratory. Because of this small derivative, there is a low probability for entering the Rydberg states via Born–Oppenheimer breakdown.

VI. CROSS SECTIONS AND RATES

In order to include the neutral Rydberg resonances, we use here the multichannel quantum defect theory that has been presented previously.[7,9] The vibrational wave functions have been calculated on a grid of 0.001 a_0 between 1.0 and 8.0 a_0 and cross sections have been calculated on a grid of 0.0001 eV from 0.0001 to 1.0 eV. Twenty ion vibrational levels have been included. The K matrix, which includes all the electronic interactions between dissociative and electron–ion states, has been calculated to second order.[9] The calculated cross section is shown in Fig. 3. The dashed line is the direct cross section calculated from Eq. (2). The solid line is the full cross section including the resonance states. The resonances here are quite sharp due to the small value for the electronic widths. The first resonance near 0.03 eV is due to the $n=7$, $v=1$ Rydberg level. Moving to higher energies, the next resonance is the $n=8$, $v=1$ level. As has been discussed previously,[7,9] the cross section takes the form of a Fano profile near each resonance. The $v=1$ resonances shown in Fig. 3 have the characteristic shape of a Fano profile with a profile index, q, having a positive value, near unity. The next resonance near 0.15 eV is $n=4$, $v=4$. Its profile is reversed relative to the $v=1$ resonances and it has a negative q. The $v=1$ resonances terminate at the $v=1$ level of the ion at 0.37 eV. Note that the full cross section is slightly below the direct cross section at low energies. This is due to the low energy wing of $n=7$, $v=1$ and to the $n=5$, $v=2$ level which falls just below threshold and has a negative Fano profile index. Except for the narrow peaks and dips due to the resonances, the full cross section and the direct cross section are quite similar. Indeed, for OH^+, indirect DR plays only a very small role.

There have been no prior calculations of cross sections or rates for the DR of OH^+. The only experimental data comes from a merged beam study[5] which reported cross sections. These experimental results are shown as the dotted line in Fig. 3. The dotted line reproduces that drawn by the experimentalists through their data points. The experimental cross section goes as $E^{-1.0}$ and agrees with the calculated energy dependence of $E^{-0.99}$ at energies away from resonances and below 0.6 eV. However, the experimentally derived cross section is about a factor of 6 higher than the cross section calculated here. The state of excitation of the OH^+ in the experiments[5] could not be determined. Indeed, the large difference between the experimental and theoretical results appears to indicate that a considerable fraction of the ion beam may have been either vibrationally or electronically excited. A possibility for the latter excitation are excited and ground vibrational levels of the $a\ ^1\Delta$ metastable state lying at 2.2 eV[12] and the higher lying $b\ ^1\Sigma^+$ state. The latter state could undergo DR along dissociative states of $^2\Sigma^+$ symmetry. Although we have not calculated a potential curve for the a state, the width matrix element for the corresponding electron–ion $^2\Pi$ state was determined in our calculations of the widths of the $^2\Pi$ states formed from the $X\ ^3\Sigma^-$ ion state. The width of the $2\ ^2\Pi$ state for coupling to the a state plus a free electron is between 3–4 times larger than that for the X state width in the region between 1.5 and 2.2 a_0. Finally, it should be noted that the merged beam measurements showed no indication of resonance structure. This is in agreement with the very narrow resonances seen here.

The DR rate has been calculated by averaging the cross section over a Maxwellian energy distribution for the electrons. The rate is shown in Fig. 4. As expected, the direct and full rates are quite similar. Indeed, for OH^+ the indirect recombination mechanism can be neglected in the calculation of the rate. Taking into account the orbital dependence of the calculated width, the recommended value for the total DR rate from $v=0$ for $10<T_e<1000$ K is $(6.3\pm0.7)\times10^{-9}\times(T_e/300)^{-0.48}$ cm^3/s.

VII. SUMMARY AND CONCLUSIONS

The DR of OH^+ with an electron is dominated by the $2\ ^2\Pi$ route which leads to O(^1D), the upper state of the red line, and hot H(^2S) with a kinetic energy of 6.1 eV. The $2\ ^2\Pi$ diabatic potential curve intersects the ion potential within the turning points of the $v=0$ level. However, the electronic capture width and the variation of the quantum defect with R are both very small yielding a small calculated recombination rate coefficient. The calculations indicate that the only

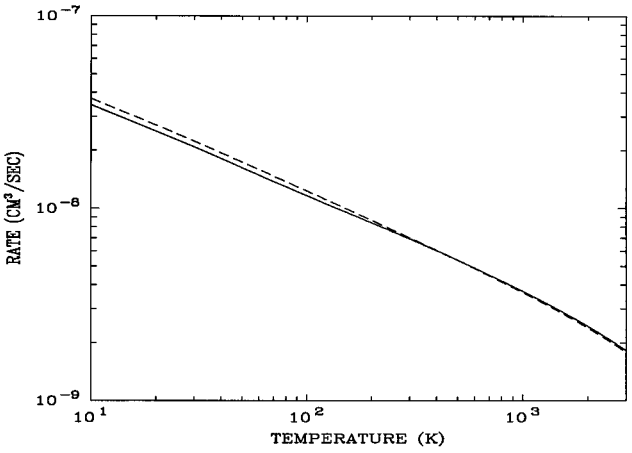

FIG. 4. The calculated direct (dashed line) and full (solid line) rates from a Maxwellian average of the cross section.

prior experimental work, a merged beam experiment, may have vibrationally or electronically excited ions in the beam in agreement with the earlier observation.[5]

ACKNOWLEDGMENTS

This research is supported by NASA Grants No. NAGW-1404 and NAGW 2832 and by NSF grant ATM-9122739. The computations were done at the Pittsburgh Supercomputer Center and the National Center for Atmospheric Research, which are both supported by NSF.

[1] W. F. Huebner, in *The Photochemistry of Atmospheres*, edited by J. S. Levine (Academic, Orlando, 1985).
[2] M. A. Coplan, K. W. Ogilvie, M. F. O'Hearn, P. Bochsler, and J. Geiss, J. Geophys. Res. **92**, 39 (1987).
[3] J. D. Richardson, A. Eviatar, and G. L. Siscoe, J. Geophys. Res. **91**, 8749 (1986).
[4] A. F. Cheng, J. Geophys. Res. **92**, 15309 (1987).
[5] P. M. Mul, J. Wm. McGowan, P. Defrance, and J. B. A. Mitchell, J. Phys. B **16**, 3099 (1983); J. B. A. Mitchell, Phys. Rep. **186**, 215 (1990).
[6] D. R. Bates, Phys. Rev. **78**, 492 (1950).
[7] A. Giusti, J. Phys. B **13**, 3867 (1980).
[8] J. N. Bardsley, J. Phys. B **1**, 365 (1968).
[9] S. L. Guberman and A. Giusti-Suzor, J. Chem. Phys. **95**, 2602 (1991).
[10] S. L. Guberman, Phys. Rev. A **49**, R4277 (1994).
[11] For a review of the DR mechanism see S. L. Guberman and J. B. A. Mitchell, *Introduction to Dissociative Recombination in Dissociative Recombination: Theory, Experiment and Applications*, edited by J. B. A. Mitchell and S. L. Guberman (World Scientific, Singapore, 1989), p. 1.
[12] K. P. Huber and G. Herzberg, *Molecular Spectra and Molecular Structure, IV. Constants of Diatomic Molecules* (Van Nostrand, Reinhold, New York, 1979).
[13] C. E. Moore, *Atomic Energy Levels*, NSRDS-NBS 35, (U.S. Government Printing Office, Washington, 1971).
[14] F. B. van Duijneveldt, Gaussian Basis Sets for the Atoms H–Ne For Use in Molecular Calculations, IBM Research Report RJ-945 (1971).
[15] P. Taylor (private communication).
[16] J. Almlöf and P. R. Taylor, J. Chem. Phys. **86**, 4070 (1987).
[17] P. E. M. Siegbahn, J. Almlof, A. Heiberg, and B. O. Roos, J. Chem. Phys. **74**, 2384 (1981).
[18] P. E. M. Siegbahn, J. Chem. Phys. **72**, 1647 (1980).
[19] E. R. Davidson, *Configuration Interaction Description of Electron Correlation in the World of Quantum Chemistry*, edited by R. Daudel and B. Pullman (Reidel, Dortrecht, 1974), p. 17.
[20] S. R. Langhoff, C. W. Bauschlicher, Jr., and P. R. Taylor, J. Chem. Phys. **91**, 5953 (1989).
[21] E. F. van Dishoeck and A. Dalgarno, J. Chem. Phys. **79**, 873 (1983) and references therein.
[22] C. Bottcher, Proc. R. Soc. London, A Ser. **340**, 301 (1974); T. F. O'Malley and S. Geltman, Phys. Rev. **137**, A1344 (1965).
[23] MOLECULE-SWEDEN is an electronic structure program written by J. Almlöf, C. W. Bauschlicher, M. R. A. Blomberg, D. P. Chong, A. Heiberg, S. R. Langhoff, P.-Å. Malmqvist, A. P. Rendell, B. O. Roos, P. E. M. Siegbahn, and P. R. Taylor.
[24] T. H. Dunning, Jr. and P. J. Hay, *Gaussian Basis Sets for Molecular Calculations in Modern Theoretical Chemistry. II. Electronic Structure: Ab Initio Methods*, edited by H. F. Schaefer III (Plenum, New York, 1977).
[25] T. H. Dunning, Jr., J. Chem. Phys. **55**, 3958 (1971).
[26] K. Kaufmann, W. Baumeister, and M. Jungen, J. Phys. B **22**, 2223 (1989).
[27] W. J. Hunt and W. A. Goddard III, Chem. Phys. Lett. **6**, 414 (1969).
[28] S. L. Guberman, *Ab Initio Studies of Dissociative Recombination in Dissociative Recombination: Theory, Experiment and Applications*, edited by J. B. A. Mitchell and S. L. Guberman (World Scientific, Singapore, 1989), p. 45.
[29] A. U. Hazi, *Molecular Resonance Phenomena, in Electron–Atom and Electron–Molecule Collisions*, edited by J. Hinze (Plenum, New York, 1983), p. 103.
[30] G. Herzberg and Ch. Jungen, J. Mol. Spectrosc. **41**, 425 (1972).